

Niels Neumann

Signal processing with optical delay line filters
for high bit rate transmission systems

Beiträge aus der Informationstechnik

Niels Neumann

**Signal processing with optical delay line filters
for high bit rate transmission systems**

 VOGT

Dresden 2011

Bibliografische Information der Deutschen Bibliothek
Die Deutsche Bibliothek verzeichnet diese Publikation in der Deutschen
Nationalbibliografie; detaillierte bibliografische Daten sind im Internet über
<http://dnb.ddb.de> abrufbar.

Bibliographic Information published by the Deutsche Bibliothek
The Deutsche Bibliothek lists this publication in the Deutsche Nationalbibliografie;
detailed bibliographic data is available in the internet at <http://dnb.ddb.de>.

Zugl.: Dresden, Techn. Univ., Diss., 2010

Die vorliegende Arbeit stimmt mit dem Original der Dissertation
„Signal processing with optical delay line filters for high bit rate transmission
systems“ von Niels Neumann überein.

© Jörg Vogt Verlag 2011
Alle Rechte vorbehalten. All rights reserved.

Gesetzt vom Autor

ISBN 978-3-938860-43-4

Jörg Vogt Verlag
Niederwaldstr. 36
01277 Dresden
Germany

Phone: +49-(0)351-31403921
Telefax: +49-(0)351-31403918
e-mail: info@vogtverlag.de
Internet : www.vogtverlag.de



Signal processing with optical delay line filters for high bit rate transmission systems

Niels Neumann

von der Fakultät Elektrotechnik und Informationstechnik
der Technischen Universität Dresden
zur Erlangung des akademischen Grades eines

Doktoringenieurs
(Dr.-Ing.)

genehmigte Dissertation

Vorsitzender: Prof. Dr.-Ing. habil. Dipl.-Math. Röbenack
Gutachter: Prof. Dr.-Ing. Schäffer
Prof. Dr.-Ing. Schmauß

Tag der Einreichung: 01.07.2010
Tag der Verteidigung: 06.12.2010

Contents

1	Introduction	1
1.1	Optical communication systems	2
1.2	Fiber impairments and equalizers	4
1.3	Outline of the thesis	6
2	Basics	7
2.1	Linear fiber transfer function	7
2.2	Fiber nonlinearities	11
2.3	Compensation of chromatic dispersion	15
2.4	Delay Line Filters	18
2.4.1	Mathematical Description	18
2.4.2	Realization options	19
2.4.3	Realization in Optics	21
3	Filter synthesis	27
3.1	Mathematical description and normalization	28
3.2	Performance limits	33
3.3	Iterative methods	36
3.3.1	Particle swarm optimization	36
3.3.2	Other iterative methods	41
3.3.3	Conclusion	44
3.4	Analytical methods for special cases	44
3.4.1	Second order dispersion compensating filter	44
3.4.2	Simplified higher order filter for dispersion compensation	49
3.4.3	Dispersion slope compensating filter	52
4	Dispersion Monitoring	61
4.1	Vestigial sideband filtering	61
4.1.1	Proof-of-concept	63
4.1.2	Electronic estimation	64
4.1.3	Conclusion	71
4.2	Nonlinear Detection	72
4.2.1	Theoretical investigation	72
4.2.2	Experiments	80

5	Control algorithms for filter adaptation	91
5.1	Control strategies	91
5.1.1	Iterative setting	93
5.1.2	Deterministic setting	94
5.1.3	Results	95
5.2	Example implementations	98
5.2.1	Wavelength centering	98
5.2.2	Autonomous dispersion compensation	100
6	Fiber optic dispersion compensator and monitor	105
6.1	Filter elements	105
6.1.1	Fiber optic couplers	105
6.1.2	Fiber delay lines	106
6.1.3	Phase shifters	106
6.2	Dispersion compensator and Monitor	107
6.2.1	Analysis and Optimization	108
6.2.2	Realization	113
6.3	Device characterization	114
6.3.1	Single channel characterization	116
6.3.2	Multi channel characterization	118
6.4	System characterization	118
6.4.1	Multi channel measurements	121
6.4.2	Single channel measurements	126
6.5	Dispersion slope compensator	128
7	Future directions	133
8	Conclusion	135

List of Figures

1.1	Concepts for tunable dispersion compensation: a) electronic compensation, electronic control signal, b) compensation in optical domain with control signal from electronics, c) compensation in optical domain with control signal from optics (before or after compensation)	5
2.1	Analogy between optical filtering with delay line filters and electronic filtering with FIR filters	20
2.2	Structure of a general fiber optic delay line filter with $(l+1) \times k$ couplers (l stages, k lines)	21
2.3	Major structures of optical delay line filters (filter order N): a) Serial structure with $(N+1) \times 2 \times 2$ couplers ($l=N$ stages, $k=2$ lines), b) Parallel structure with $2 \times (N+1) \times (N+1)$ couplers ($l=1$ stage, $k=N+1$ lines)	23
2.4	Minimum power coupling ratio with respect to number of coupler output ports	26
3.1	Dispersion function of one zero with $\rho_{0,k}$ as parameter	31
3.2	Maximum filter order of the optical filter needed for the compensation of the dispersion of 500 km SMF for a 10 Gbit/s NRZ signal depending on the realization FSR	36
3.3	Principle of one iteration step of particle swarm optimization	39
3.4	Penalties of filters generated with PSO for filter order $N = 4$ and $N = 10$	42
3.5	General optical delay line filter of order $N = 2$	45
3.6	General principle of generating constant dispersion out of two sawtooth-like functions	50
3.7	Performance of the simplified analytical method for higher order filters: a) dependency of produced dispersion on the filter order (RBWU=50%), b) dependency of produced dispersion on the relative bandwidth ($N=4$)	53
3.8	General optical delay line filter of order $N = 1$	54

3.9	One stage dispersion slope compensator: a) bandwidth with respect to power coupling coefficient, b) Slope with respect to power coupling coefficient	56
3.10	Principle of generating an arbitrary sawtooth out of unsymmetrical sawtooths	57
3.11	Maximum dispersion slope with respect to filter order N and relative bandwidth RBWU at fitness 0.15	60
4.1	Setup of optical delay line filter	62
4.2	Measured transfer functions of the passband, LSB and USB filter output ports	63
4.3	Proof-of-concept measurement setup	64
4.4	Eye diagrams of the LSB, USB and passband signal at the presence of 80 ps/nm dispersion	65
4.5	Estimated dispersion vs. fiber dispersion for a 10 Gbit/s NRZ signal LSB and USB measurement	65
4.6	Experimental setup	66
4.7	Influence of the filter transfer function on the normalized mixer output voltage (filter input power: 2 dBm)	68
4.8	Influence of noise and nonlinearities on the mixer output voltage (filter state: 36° , filter input power: 2 dBm)	69
4.9	a) Monitor port 1 and monitor port 2 transfer functions for different minimal transmission t_{min} , b) Normalized mixer output voltage for different minimal transmission t_{min}	70
4.10	a) Spectra at the filter's three output ports, b) Measured mixer output voltage for two different measurement configurations	71
4.11	Simulation setup for nonlinear output calculation and amplitude distribution simulation	72
4.12	Constellation diagrams including transitions and setup of a) DPSK, b) DQPSK (ideal PM setup), c) RZ-DQPSK and d) DQPSK (MZM setup) transmitters	74
4.13	Output signal of the nonlinear detector for different modulation formats in the presence of dispersion	75
4.14	Field amplitude level distribution and resulting normalized output of the nonlinear detector (normalized nonlinear output) for DQPSK (MZM) modulation format under presence of chromatic dispersion	77
4.15	Experimental setup for dispersion monitoring using nonlinear detection	80
4.16	Bias points and driving voltage for a) NRZ and b) RZ pulse generation	81
4.17	Incident CW power versus nonlinear detector output	83

4.18	Adjusting the number of counts according to small power changes with linear approximation	84
4.19	Dependency of the nonlinear output on the EDFA amplification factor at 6 dBm, 10 dBm and 14 dBm EDFA output power . . .	86
4.20	Dependency of nonlinear output on dispersion (at constant EDFA input and output power): histogram estimation of nonlinear output and photon counter output for a) NRZ and b) inverse RZ .	87
4.21	Dependency of nonlinear output on dispersion (at constant EDFA input and output power): Different modulation formats (NRZ with positive and negative chirp, RZ and inverse RZ)	89
5.1	Simulation setup for the evaluation of control strategies	92
5.2	Control behavior of dispersion compensating device	93
5.3	Gradient analysis for iterative adjustment of the dispersion compensator control variable	94
5.4	Iterative control behavior with a fixed step size of 5° , 10° and 20°	95
5.5	Iterative control behavior with an adaptive step size of maximal 50° and maximal 100° compared with 10° fixed step size	97
5.6	Deterministic vs. iterative control at residual dispersion step . .	97
5.7	Measured passband (10 ps/nm dispersion, 50 GHz FSR), monitor 1 and monitor 2 transfer function and 10 Gbit/s NRZ spectrum	98
5.8	Monitor 1 and monitor 2 output power with respect to spectral position of the signal (normalized to channel bandwidth)	99
5.9	Flow chart of wavelength centering algorithm	99
5.10	Setup for autonomous dispersion compensator using monitor ports	101
5.11	Flow chart of autonomous dispersion compensation algorithm . .	102
5.12	Filter output powers and values of the temperature controllers setting φ_1 and φ_2 with respect to time in an air-conditioned environment	104
6.1	Dependency of the phase on the temperature of the fiber heating element	108
6.2	Simulation setup for optical bandwidth and group delay ripple border conditions	108
6.3	Influence of the 3 dB bandwidth on the bit error rate	109
6.4	Bit error rate with respect to ripple amplitude, sinusoidal ripple is present over the full FSR	110
6.5	Bit error rate with respect to spectral position of the ripple (10 ps sinusoidal ripple with 10 GHz bandwidth shifted inside the spectrum, FSR of 100 GHz with the carrier located at 50 GHz) . . .	110

6.6	Coupling ratio with respect to dispersion tuning range for a filter with 100 GHz FSR, an optical bandwidth of 35 GHz and a group delay ripple of 10 ps	111
6.7	Tuning behavior of the optimized dispersion compensator using the coupling coefficient $\kappa_{opt} = 0.69$	112
6.8	a) Setup for measuring dispersion compensator characteristics b) Algorithm for automatic measurement	115
6.9	Single channel measurement results for a 100 GHz FSR dispersion compensation filter	117
6.10	Simulation results and measurement for dispersion compensator for different filter states	119
6.11	Multi channel measurement results for a 100 GHz FSR dispersion compensation filter: Filter state 29° C	120
6.12	104 superimposed channels (83.2 nm) of a 100 GHz FSR dispersion compensation filter: Filter state 29° C	121
6.13	Spectra after the dispersion compensator: Center frequency optimized for channel 2, out-of-grid channel 8 and automatically wavelength-centered	123
6.14	Channel powers after the dispersion compensator: Center frequency optimized for channel 2, out-of-grid channel 8 and automatically wavelength-centered	124
6.15	Channel insertion loss due to the dispersion compensator: Center frequency optimized for channel 2, out-of-grid channel 8 and automatically wavelength-centered	124
6.16	Additional insertion loss per channel when tuning the filter	125
6.17	Setup for single channel eye diagram measurements	126
6.18	Eye diagrams: 2.5 Gbit/s test signal, in ADVA FSP II before multiplexing filter, after demultiplexing filter (with and without dispersion compensator)	127
6.19	Spectra with and without dispersion compensator: a) 2.5 Gbit/s NRZ (ADVA FSP II) after demultiplexing filter, b) 10 Gbit/s NRZ (Anritsu MP1570A)	127
6.20	Setup for single channel bit error rate measurements	128
6.21	Bit error rate with respect to received optical power (with and without dispersion compensator)	129
6.22	Measured dispersion slope compensator with maximum slope and FSR=100 GHz	130
6.23	Measured dispersion slope compensator with maximum bandwidth and FSR=100 GHz	131

List of Tables

2.1	Dispersion compensation methods	16
2.2	Dispersion compensation methods (continued)	17
3.1	Conversion between the normalized and not normalized values for a free spectral range FSR=100 GHz and center wavelength $\lambda_{center}=1550$ nm	30
4.1	Dispersion tolerance for analyzed modulation formats for 100 Gbit/s	73
5.1	Properties of control algorithm classes	96
6.1	Channels in WDM link Berlin-Hannover-Darmstadt at Berlin Tx	122
6.2	Key properties of the realized demonstrators	132

Nomenclature

ADC	Analog-to-digital conversion
ASIC	Application specific integrated circuit
AWG	Arrayed waveguide grating
BER	Bit Error Rate
CD	Chromatic dispersion
DAC	Digital-to-analog conversion
DCF	Dispersion compensation fiber
DFB	Distributed feed-back
DPSK	Differential phase-shift keying
DQPSK	Differential quaternary phase-shift keying
ECL	External cavity laser
EDFA	Erbium Doped Fiber Amplifier
FBG	Fiber Bragg Grating
FIR	Finite impulse response
FPGA	Field-programmable gate array
FSR	Free Spectral Range
GVD	Group velocity distortion
I/O	Input/output
IIR	Infinite impulse response
ITU	International telecommunication union
LSB	Lower side band
MZM	Mach-Zehnder modulator
NRZ	Non-return-to-zero
OSNR	Optical signal-to-noise ratio
OVA	Optical vector analyzer
PDL	Polarization Dependent Loss
PHASAR	Phased array
PM	Phase modulator
PMD	Polarization mode dispersion
PRBS	Pseudo-random binary sequence
PSO	Particle Swarm Optimization
RBWU	Relative bandwidth used
ROADM	Reconfigurable optical add-drop multiplexer
RZ-DQPSK	Return-to-zero differential quaternary phase-shift keying
SBS	Stimulated Brillouin Scattering

SMF	Single Mode Fiber
SPM	Self-Phase-Modulation
SRS	Stimulated Raman Scattering
TDC	Tunable dispersion compensator
USB	Upper side band
VIPA	Virtual image phased array
VOA	Variable Optical Attenuator
WDM	Wavelength division multiplex
XPM	Cross-Phase-Modulation

1 Introduction

Over the course of the past decades, the global communication system has become a central part of people's everyday lives. These days, various applications run on top of the internet providing reams of services that connect people across borders and despite different time zones. Among the various applications that can be used over the internet there are a few ones that set new demands for the transmission technologies. Where e-mail, mostly-text WWW and instant messaging are frugal with respect to bandwidth and latency the new development towards "one line for everything" can be identified as one key driver.

The starting convergence of telephone, TV / video-on-demand and internet to one IP-based service is dominated by the bandwidth needs of the video segment. Now found all over the world, this new type of service was first introduced in Asia (Japan and Korea). In Germany, Deutsche Telekom started the so-called "Triple Play" service in mid 2006. Now, it is becoming more widely available in more and more cities. World wide web based video broadcasting has also become increasingly popular. User-generated content sites like Youtube attract a constantly growing number visitors. Television and radio stations also use the internet to broadcast their daily programs. For example, NBC in the United States, BBC in Great Britain and the major channels in Germany have created media centers where internet users can access clips of their programs at any time.

New applications are another driver for the fixed lines. Working together over long distances will be easier using video conferences and virtual private networks that can reach over continents. International teams will be able to access and process data stored in one central place in their private network (which is still part of the internet).

Data storage, software and services migrate to servers in the internet - "the cloud". Giants of the internet industry like Google, Amazon or IBM already offer cloud computing services such as Google Docs, Amazon EC2 and IBM Smart Business services.

For elderly persons or people with poor health, electronic health monitoring could ensure a better care and treatment. The examples mentioned previously generate new needs for the bandwidth and robustness of the installed broadband line.

By using new classes of devices such as smartphones (e.g. the iPhone) people can constantly be connected to the internet, and from a multitude of locations.

Mobile phones delocalized voice conversations and introduced texting. Smart-phones will delocalize e-mailing, browsing, instant messaging and downloading and will also introduce new forms of communication. Following the tendency to ubiquitous computing, a multitude of connected devices will form the internet of things.

All things considered, a fast network access is required in a higher number of locations. In today's society, the number of installed WiFi hotspots is always increasing. UMTS coverage and speed are also on the rise. Its successor, LTE, is already in the starting blocks and is being developed. Wireless access points have to be connected to a backbone to ensure a broadband connection. Thus, backbone capacity upgrades are required in the internet.

The applications discussed previously set the requirement for a higher access speed. Latency, however, is not a big issue. There are only a few critical applications like telephony, video conferences and online games which truly require a low latency. Today's latency provides an acceptable quality of service as experienced when using voice-over-IP. Increasing line speed, however, is the main challenge and covers more than simply providing the home user with a faster access. A higher speed for end users aggregates to a higher overall traffic in the backbone and a higher throughput in the exchange points. This growth is already in progress. For example, in the Frankfurt exchange point, within two years, the traffic increased by more than 400%.

On the other hand, the customer sets tight economic boundaries for the carriers. The end-user is not willing to increase cost of his communication access although they wish to have speed upgrades and additional traffic. Hence, the costs per bit have to be lowered in a joint effort of network operators, system vendors, equipment manufacturers and researchers.

1.1 Optical communication systems

Optical communication systems are the technological basis for this development. Only fibers can provide the huge bandwidth that is required. Forming the backbone of the international communications network, photonics helps to connect continents, countries and people. The answer to these challenges is increasing the efficiency of the transmission. The line speed of the WDM channels was increased and will be increased: The upgrade path goes from legacy 2.5 Gbit/s lines to 10 Gbit/s, 40 Gbit/s and up to 100 Gbit/s which is currently in standardization. For 100 Gbit/s systems, different approaches are followed [41]. It can be distinguished between parallel and serial concepts.

The straight-forward way to 100 Gbit/s is the bundling of multiple wavelength channels of lower data rates (e.g. 10x10 Gbit/s or 4x25 Gbit/s) to a 100 Gbit/s super channel. Indeed, this approach was the first to be standardized and also

the first to be commercially available. However, there is no gain in terms of spectral efficiency. Just the handling of the channels and the multiplexing changed in comparison to traditional (D)WDM systems.

OFDM with its numerous sub-carriers can be also interpreted as a parallel approach. OFDM offers some advantages in terms of scalability. It is proposed that the trade-off between the tolerance to impairments such as chromatic dispersion or polarization mode dispersion and transmission length can be adjusted in a wide range of operation. Nonetheless, OFDM has high requirements to signal processing power. Fast ADCs and DACs as well as high-throughput ASICs are needed. Also, nonlinearities and the laser linewidth are issues. First real-time receiver implementations using FPGAs were demonstrated in the lab at multi-Gbit/s data rates. There is still a long way to 100 Gbit/s OFDM systems.

Serial 100 Gbit/s systems providing one optical channel with this high data rate can be classified by the spectral efficiency. Generally speaking, increasing the spectral efficiency results in a higher hardware effort. There is always a compromise to find between the complexity in the electrical domain and in the optical domain.

The simplest optical systems operating at about 1 bit/s/Hz. In that case on-off-keying (OOK), differential phase-shift keying (DPSK) or duobinary formats are used. Challenges are the high cut-off frequency needed in the electrical domain for components such as the optical modulator, the electrical amplifiers, multiplexers and so on. These components are available for lab applications at a high price. Due to the low spectral efficiency, a 100 GHz or even a 200 GHz channel grid have to be considered.

Adding polarization multiplexing to the OOK, DPSK, ... formats or using (differential) quaternary phase shift keying ((D)QPSK) leads to setups with doubled spectral efficiency of 2 bit/s/Hz. Adding complexity in the optics (polarization splitters and combiners or 90° hybrids) relaxes the demands in the electrical domain. Electronics from 40 Gbit/s products can be re-used lowering the expenses. For these systems, still cost-effective direct detection at the receiver side may be an option. 100 GHz or even 50 GHz channel grids are possible.

Doubling again the spectral efficiency (4 bit/s/Hz) pushes the fiber even more toward its capacity limit. This enables 50 GHz DWDM channel grids and actually a 25 GHz spacing becomes possible. Using polarization multiplexed QPSK requires much more complexity in the optical domain: polarization splitters and combiners and 90° hybrids in conjunction with coherent detection have to be used. In the electrical domain, the constraints for the cut-off frequency of the electronics are more relaxed, again. This means, components of 40 Gbit/s systems can be reused once more. On the other hand, high speed ASICs are needed for the processing of the raw data streams acquired by the ADCs after the coherent detection. With all the information from the optical domain available, all linear impairments theoretically can be compensated. The first serial 100 Gbit/s

system that was commercially deployed used polarization multiplexed QPSK as modulation format. In December 2009, Verizon put a 100 Gbit/s link on a single wavelength between Paris and Frankfurt / Main into operation. That system was provided by Nortel (now acquired by Ciena).

1.2 Fiber impairments and equalizers

Where the fiber could be regarded as a flat channel for the first optical transmission systems wavelength multiplexing and increasing line rates made it necessary to take more and more physical effects into account: Nonlinear effects like Self-Phase-Modulation (SPM) and Cross-Phase-Modulation (XPM) are now considered in the system design and Chromatic Dispersion (CD) is compensated by special Dispersion Compensating Fibers (DCF) or by Fiber Bragg Gratings (FBG). Polarization Mode Dispersion (PMD) is also a big issue.

When the line rates are increased to 40 Gbit/s and higher static chromatic dispersion compensation is not enough. The modulation format's intrinsic tolerance for dispersion decreases quadratically with the symbol rate. Thus, environmentally induced chromatic dispersion fluctuations may exceed the dispersion tolerance of the modulation formats. This makes an adaptive dispersion compensation necessary implying also the need for a monitoring scheme to steer the adaptive compensator. Legacy links that are CD-compensated by DCFs can be upgraded with residual dispersion compensators to make them ready for high speed transmission.

The generation of the feedback signal to the tunable dispersion compensator (TDC) and the compensation itself may be performed in the electrical domain as well as in the optical domain.

Electronic compensation and also the electronic generation of the feedback signal can only be performed at the receiver side for a single channel. Using direct detection decreases the performance as the phase information of the optical field is lost. Coherent detection enables the full compensation of all linear impairments at the cost of a much more complicated receiver architecture. The power consumption of such an electronic equalizer becomes more and more an issue with increasing line rates because the power dissipation increases with the operating frequency. Furthermore, the required computation power is also challenging.

Another approach is the optical compensation of link impairments. The optical compensation is independent from the line rate. Hence, increasing the data rates is inherently supported. Optical compensators can be built WDM ready compensating multiple channels at once. All this enhances the energy efficiency pioneering green IT.

The control information for the optical compensator can still be acquired in the

electrical domain. In that case, high speed electronics is at least partly needed for eye opening or pulse width estimation. Using the receiver BER as a measure is also an option. Yet, with only reduced or indirect information available, finding the optimal setting for the TDC might be hard. Again, the equalizer is restricted to be used at the receiver.

That might be overcome by directly obtaining the control information from the optical domain. Consequently, this kind of compensators can be used anywhere in the network, not just at the receiver. True autonomous operation is provided while the advantages of optical compensation (power efficiency, WDM operation, ...) are maintained.

Figure 1.1 illustrates these three options.

The transmitter can also be modified: The transmitted signal can be pre-distorted so that an error-free signal is received. However, providing a feedback signal to the transmitter is challenging and the implementation of the high-speed electronics needed for the pre-distortion filter has the same constraints as electronic post-compensation at the receiver. Hence, this approach will not be regarded here.

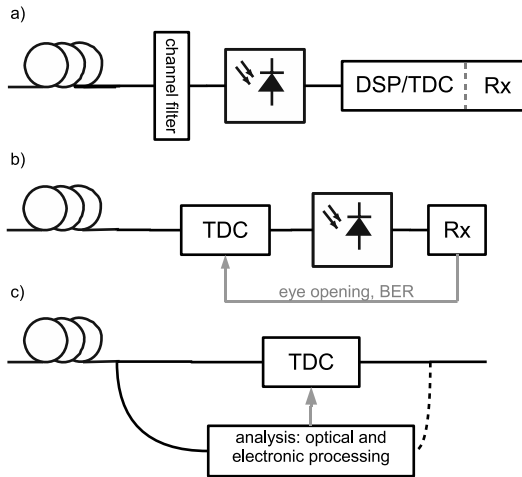


Figure 1.1: Concepts for tunable dispersion compensation: a) electronic compensation, electronic control signal, b) compensation in optical domain with control signal from electronics, c) compensation in optical domain with control signal from optics (before or after compensation)

1.3 Outline of the thesis

Aspects of this widespread topic are addressed in this thesis. In the next chapter, the basic properties of the impairment that will be dealt with - chromatic dispersion - will be discussed. Also, nonlinear effects and dispersion compensation possibilities are reviewed and delay line filters as one compensation method will be introduced.

Chapter three deals with the synthesis of such delay line filters. Iterative and analytical methods that produce the coefficients for dispersion (and also dispersion slope) compensating filters were researched.

As important as the compensation of dispersion is the estimation of the dispersion of a signal. In chapter four, two dispersion monitoring methods were investigated. Using delay line filters, the vestigial sidebands of a signal can be used to measure the dispersion. Alternatively, nonlinear detection can be used to estimate the pulse broadening which is caused mainly by dispersion.

With dispersion compensation and dispersion monitoring, dispersion compensators can be adapted to the signal's impairment. Chapter five deals with control algorithms for filter tuning. Special properties of the filter in conjunction with an analytical description can be used to provide a fast and reliable control algorithm for dispersion setting and wavelength adjustment of the dispersion compensation filter.

Prototypes of such fiber optic chromatic dispersion and dispersion slope compensation filters were manufactured and characterized. Chapter six deals with the optimization and realization of these filters. Furthermore, the device and system characterization of the prototypes is presented.

Finally, in the last two chapters, future directions are discussed and a conclusion is given.

2 Basics

Present long-haul high speed systems use optical single mode fibers (SMF) as medium to transmit data. Using decent launch powers, nonlinearities of this medium can be neglected. Under these assumptions, the single mode fiber is a linear medium. Describing the fiber with the wave equation explains the dispersive effects that limit the transmission length. Anyhow, under certain conditions nonlinearities have to be taken into account. Therefore, an overview of cause and effect of nonlinearities is given and self-phase modulation (SPM) is focused.

Being the major impairment of the linear fiber, chromatic dispersion has to be compensated. Consequently, a review of dispersion compensation methods will follow. One possibility for adaptive dispersion compensation is the use of delay line filters. These delay line filters can be realized as optical delay line filters or as digital FIR filters. Both realizations are equivalent. However, the differences due to the realization in optical domain or in electrical domain will be addressed. Finally, the focus will be on optical delay line filters and their mathematical description.

2.1 Linear fiber transfer function

The fiber can be treated as a linear dispersive medium satisfying the wave equation with the electric field E , the refractive index n , the speed of light in vacuum c and the time t

$$\Delta E = - \left(\frac{n}{c} \right)^2 \frac{\partial^2 E}{\partial t^2}. \quad (2.1)$$

Using the field

$$E(z, t) = A(z, t)F(x, y)e^{-j(\beta_0 z - \omega_0 t)} \quad (2.2)$$

with the slowly varying envelope $A(z, t)$, the mode field $F(x, y)$ oscillating at the carrier frequency ω_0 and propagating with β_0 in the direction of z the second derivatives needed for (2.1) can be calculated¹

¹This approach can be applied to optical small bandwidth systems. All optical transmission systems belong to that category using a carrier frequency of 200 THz and a signal bandwidth of less than 1 THz.

$$\frac{\partial^2 E(z, t)}{\partial z^2} = F(x, y) e^{-j(\beta_0 z - \omega_0 t)} \left(\frac{\partial^2 A(z, t)}{\partial z^2} - 2j\beta_0 \frac{\partial A(z, t)}{\partial z} + \beta_0^2 A(z, t) \right) \quad (2.3)$$

$$\frac{\partial^2 E(z, t)}{\partial t^2} = F(x, y) e^{-j(\beta_0 z - \omega_0 t)} \left(\frac{\partial^2 A(z, t)}{\partial t^2} + 2j\omega_0 \frac{\partial A(z, t)}{\partial t} - \omega_0^2 A(z, t) \right). \quad (2.4)$$

Due to the slowly varying envelope $A(z, t)$ of the signal with a bandwidth that is much smaller than its carrier frequency following estimations can be made

$$\frac{\partial^2 A(z, t)}{\partial z^2} \ll -2j\beta_0 \frac{\partial A(z, t)}{\partial z} + \beta_0^2 A(z, t) \quad (2.5)$$

$$\frac{\partial^2 A(z, t)}{\partial t^2} + 2j\omega_0 \frac{\partial A(z, t)}{\partial t} \ll \omega_0^2 A(z, t) \quad (2.6)$$

leading to the differential equation

$$-2j\beta_0 \frac{\partial A(z, t)}{\partial t} + \beta_0^2 A(z, t) = \left(\frac{n\omega_0}{c} \right)^2 A(z, t). \quad (2.7)$$

Now, a Fourier transform is applied to describe the linear dispersive fiber in frequency domain. The frequency dependency of the refractive index $n(\omega)$ causes the dispersive behavior by leading to a frequency dependent propagation constant

$$\beta(\omega) = \frac{n(\omega)\omega_0}{c}. \quad (2.8)$$

Inserting (2.8) into the Fourier-transformed differential equation (2.7) leads to

$$0 = \frac{\partial A(z, \omega)}{\partial z} + \frac{j}{2\beta_0} (\beta^2(\omega) - \beta_0^2) A(z, \omega). \quad (2.9)$$

The changes in refractive index and therefore in the propagation constant are relatively small ($\beta(\omega) \approx \beta_0$) so that the approximation

$$\beta(\omega)^2 - \beta_0^2 = (\beta(\omega) - \beta_0)(\beta(\omega) + \beta_0) \approx (\beta(\omega) - \beta_0)2\beta_0 \quad (2.10)$$

can be used simplifying the differential equation

$$0 = \frac{\partial A(z, \omega)}{\partial z} + j(\beta(\omega) - \beta_0) A(z, \omega). \quad (2.11)$$

Now, the propagation constant is expanded as a Taylor series around the center frequency ω_0 with $\omega' = \omega - \omega_0$

$$\beta(\omega') = \beta_0 + \frac{\partial\beta}{\partial\omega}\omega' + \frac{\partial^2\beta}{2\partial\omega^2}\omega'^2 + \frac{\partial^3\beta}{6\partial\omega^3}\omega'^3 + \dots \quad (2.12)$$

The linear term represents the group delay² τ , the quadratic term is the first order group velocity distortion (leading to the chromatic dispersion) and the cubic term is the second order group velocity distortion (leading to the dispersion slope). In most cases the higher order (> 3) group velocity distortions (dispersions) are not of interest. For the sake of simplification, β_k is introduced for the Taylor series approximation factor of order k

$$\beta_1 = \frac{\partial\beta}{\partial\omega} \quad (2.13)$$

$$\beta_2 = \frac{\partial^2\beta}{2\partial\omega^2} \quad (2.14)$$

$$\beta_3 = \frac{\partial^3\beta}{6\partial\omega^3} \quad (2.15)$$

\vdots

From the system point of view, chromatic dispersion D and dispersion slope S are more commonly used than the group velocity distortions (GVD). They can be calculated from β_2 and β_3 , respectively

$$D = -\frac{2\pi c}{\lambda^2}\beta_2 \quad (2.16)$$

$$S = \left(\frac{2\pi c}{\lambda^2}\right)^2\beta_3 + \frac{4\pi c}{\lambda^2}\beta_2. \quad (2.17)$$

Concluding, the linear fiber has two effects on the transmitted signal: It is attenuated and it suffers from dispersion. The optical transmission systems regarded in this thesis operate in the third optical transmission window of the single-mode fiber at a wavelength of about 1550 nm. There, a typical value for SMF attenuation is 0.2 dB/km. In the linear case, this attenuation can be treated independently from the dispersive effects. Chromatic dispersion is one of the limiting factors for high bit rate optical transmission systems. A SMF has a typical chromatic dispersion of 17 ps/(nm km), respectively $\beta_2 = -20$ ps²/km. The chromatic dispersion causes a pulse broadening due to different propagation speeds for the different spectral components of the pulse. This limits the

²the reciprocal value of the group velocity $v_{gr} = \frac{1}{\tau}$

transmission distance depending on the pulse shape and chirp used because of inter-symbol interference.

The slowly varying envelope $A(z, t)$ at the transmitter ($z = 0$) can include frequency changes with respect to the carrier frequency³ ω_0 . Assuming gaussian pulses⁴, the complex envelope at the transmitter (in equation (2.2)) can be written as

$$A(t) = A_0 e^{-\frac{t^2}{2T_0^2}} e^{-j\frac{Ct^2}{T_0^2}}. \quad (2.18)$$

The gaussian pulse shape is defined by $A_0 e^{-\frac{t^2}{2T_0^2}}$ with the half 1/e-pulse width T_0 . The chirp is characterized by the chirp parameter C leading to the time-dependent frequency offset $e^{-j\frac{Ct^2}{T_0^2}}$. Propagating this pulse shape along the fiber using equation (2.2) leads to the pulse width after the fiber length L [49]

$$T(L) = T_0 \sqrt{\left(1 + \frac{C\beta_2 L}{T_0^2}\right)^2 + \left(\frac{\beta_2 L}{T_0^2}\right)^2}. \quad (2.19)$$

For $C\beta_2 > 0$ the pulse broadening is increased by the chirp. On the other hand, $C\beta_2 < 0$ first compresses the pulse (decreases the pulse width). At the fiber length

$$L_{min} = -\frac{CT_0^2}{\beta_2(1 + C^2)} \quad (2.20)$$

the pulse has its minimal pulse width. For longer fibers, the pulse broadens again. Compared to the chirp-free case, this broadening is also increased by the chirp.

A measure for the pulse broadening is the dispersion length L_D . At the dispersion length, the pulse broadened to $\sqrt{2}$ of its original width T_0 . For the chirp-free case ($C = 0$), the dispersion length calculates to

$$L_D = \frac{T_0^2}{|\beta_2|}. \quad (2.21)$$

Taking into account the chirp, the dispersion length is reduced to

$$L_{D,C} = \frac{L_D}{\sqrt{1 + C^2}}. \quad (2.22)$$

³Chirp may be caused by direct modulated lasers but also by external modulators. It can be used purposefully or be an undesired effect.

⁴Unlike other pulse shapes such as raised cosine that are used in deployed systems, Gaussian pulses do not change their shape under the influence of dispersion. This eases the mathematical description of the pulse broadening process.

Generally, the dispersion length L_D decreases quadratically with decreasing pulse width T_0 , i. e. for transmission at higher bit rate with more narrow pulses the transmission length without dispersion compensation gets very small. Even small dispersion values may lead to link outages. Thus, dispersion compensation is unavoidable.

2.2 Fiber nonlinearities

When the launch powers into the fiber are increased, nonlinearities due to the high power density have to be dealt with. The nonlinear processes can be categorized into stimulated scattering and into the optical Kerr effect because of a changing refractive index in the fiber.

Contrary to the change of the refractive index, the stimulated scattering has a threshold power. Stimulated Raman scattering (SRS) and stimulated Brillouin scattering (SBS) are avoided in the optical communication systems by not exceeding the threshold power. Note that these effects can also be used for optical amplification.

The power-dependent refractive index in the fiber leads to self-phase modulation (SPM), cross-phase modulation (XPM) and four wave mixing (FWM). Self-phase modulation may occur in single channel systems. The power of the signal leads to a nonlinear phase change of the signal. Cross-phase modulation is similar to self-phase modulation but is caused by the power fluctuations of neighboring channels in WDM systems. Four-wave mixing adds new spectral lines and can be compared to third-order intermodulations in the electrical domain.

For the mathematical description, the general vectorial wave equation has to be used [49]

$$\nabla \times \nabla \times E(r, t) + \frac{1}{c^2} \frac{\partial^2 E(r, t)}{\partial t^2} = -\mu_0 \frac{\partial^2 \Psi(r, t)}{\partial t^2} \quad (2.23)$$

where $E(r, t)$ is the electric vector field and $\Psi(r, t) = \varepsilon E(r, t)$ is the polarization. Ψ can be expanded to the powers of E using the susceptibility tensors $\chi^{(n)}$

$$\Psi = \varepsilon_0 \left(\chi^{(1)} E + \chi^{(2)} EE + \chi^{(3)} EEE + \dots \right) . \quad (2.24)$$

The first term $\chi^{(1)} E$ covers the linear case and the second term $\chi^{(2)} EE$ can be neglected for silica glass fibers due to the fiber's inversion symmetry [49]. Hence, the third term of this expansion $\chi^{(3)} EEE$ leads to the contributions of the nonlinear processes. Therefore, the polarization can be divided in its linear and its nonlinear contributions

$$\Psi = \Psi_{lin} + \Psi_{nonlin} . \quad (2.25)$$

The contribution of the nonlinear polarization Ψ_{nonlin} is treated as a small variation compared with the linear polarization Ψ_{lin} . This is a plausible assumption because the refractive index change induced by nonlinearities is smaller than 10^{-6} . Furthermore, the approximation that the polarization remains constant over the fiber length leads to a scalar approach. Note that the polarization only remains constant for polarization maintaining fibers. For the effects considered in this thesis, this approach is known to produce reasonable results for the standard single-mode fiber and the dispersion compensating fiber [1]. Again, like in the linear fiber transfer function, optical small bandwidth systems with a bandwidth of less than 1 THz are regarded.

A nonlinear contribution to the dielectric constant can be expressed. In terms of optics, the refractive index is used. The resulting refractive index [1]

$$n' = n + n_2 |E|^2 \quad (2.26)$$

consists of the linear (power-independent) part n and the nonlinear part n_2 . The resulting absorption consisting of the linear part α and the nonlinear part α_2 is expressed in a similar way [1]

$$\alpha' = \alpha + \alpha_2 |E|^2. \quad (2.27)$$

Having a much smaller influence as the refractive index change, the nonlinear influence on attenuation is neglected. For the time domain description, the nonlinear parameter γ is introduced [1]

$$\gamma(\omega_0) = \frac{n_2(\omega_0)\omega_0}{A_{eff}c} \quad (2.28)$$

setting the relationship between the power dependent and also frequency dependent refractive index change $n_2(\omega_0)$ and the effective mode area [1]

$$A_{eff} = \frac{\left(\int_{-\infty}^{\infty} \int_{-\infty}^{\infty} |F(x, y)|^2 dx dy \right)^2}{\int_{-\infty}^{\infty} \int_{-\infty}^{\infty} |F(x, y)|^4 dx dy} \quad (2.29)$$

of the fiber at the frequency ω_0 with the field distribution $F(x, y)$. Using the retarded time

$$t' = t - \frac{z}{v_{gr}} = t - \beta_1 z \quad (2.30)$$

means following a pulse over its propagation with the group velocity v_{gr} . For pulse widths of more than 5 ps, this leads to the differential equation [1]

$$0 = j \frac{\partial A}{\partial z} + j \frac{\alpha}{2} A - \frac{\beta}{2} \frac{\partial^2 A}{\partial t'^2} + \gamma |A|^2 A. \quad (2.31)$$

Compared with the differential equation (2.9) for the linear fiber, this equation contains the nonlinear contributions and also the attenuation. The attenuation influences the nonlinear effects because the pulse power is reduced with increasing fiber length. The effective length

$$L_{eff} = \frac{1 - e^{-\alpha L}}{\alpha} \quad (2.32)$$

describes the fiber length of an unattenuated ($\alpha = 0$) fiber with the same nonlinear impact as an attenuated fiber. Introducing L_{eff} removes the attenuation dependency from the differential equation (2.31) leading to the most simple equation dealing with third order nonlinear effects in the fiber. This special case was intensively studied and is referred to as nonlinear Schrödinger equation (NLS)

$$0 = j \frac{\partial A}{\partial z} - \frac{\beta}{2} \frac{\partial^2 A}{\partial t'^2} + \gamma |A|^2 A. \quad (2.33)$$

The interaction of attenuation, dispersion and nonlinearities in the fiber are commonly taken into account using numerics. The split-step Fourier method is the most common approach in numerical calculations and simulations. The fiber is segmented in small sections of Δz where it can be assumed that nonlinearity and dispersion act independently from each other. In a first step, only the nonlinearity is evaluated in time domain. In a second step, dispersion is applied in frequency domain⁵. That way, section by section in Δz steps the pulse is propagated through the fiber.

Assuming Gaussian pulses, equation (2.31) can be evaluated for the pulse broadening, again. While the linear case in chapter 2.1 lead to the dispersion length L_D (equation (2.21)), the nonlinearities now introduce a power dependent nonlinearity length [1]

$$L_{NL} = \frac{1}{\gamma P_0} \quad (2.34)$$

where the pulse is broadened to $\sqrt{2}$ of its original length due to the peak power P_0 of the pulse. Using the characteristic lengths L_D and L_{NL} , different cases can be distinguished.

If the fiber length L is much shorter than L_D and L_{NL} , both effects can be

⁵The dispersive impact is calculated more quickly in frequency domain being a complex multiplication. Staying in time domain would result in requiring a convolution which is more lengthy than two Fourier transforms and one complex multiplication.

neglected. Anyway, this effect is not of interest because the dispersion length becomes very short for high bit rate systems. Taking the example of the commercially deployed 100 Gbit/s links using polarization multiplexed DQPSK signals⁶, the dispersion length in SMF is about 80 km, for DCF 16 km. For a 100 Gbit/s NRZ approach⁷, the dispersion length would be only 5 km for SMF and 1 km for DCF.

If the nonlinear length is much bigger than the dispersion length, the fiber can be regarded as linear dispersive medium. Revisiting the examples, 100 Gbit/s polarization multiplexed DQPSK with 0 dBm launch power leads to a nonlinear length of 500 km in standard single mode fiber at a nonlinear parameter $\gamma \approx 2/(\text{W km})$ [1]. Feeding 0 dBm in a dispersion compensating fiber with $\gamma = 6/(\text{W km})$ [35] still leads to 167 km for L_{NL} . 100 Gbit/s NRZ with balanced zeros and ones leads to lower values for L_{NL} of 250 km for SMF and 83 km for DCF. Yet, also for DCF, the dispersive effect is dominating because of the as well decreased dispersion length L_D .

Increasing the launch powers induces the third case. The dispersion length and the nonlinearity length are about the same. This means, chromatic dispersion and nonlinearities interact with each other and can not be treated separately. In such a situations, for example solitons can be created. Hence, extensive numerical calculations employing e.g. the split-step Fourier method have to be used. For the 100 Gbit/s polarization multiplexed DQPSK, the launch power for $L_D = L_{NL}$ would be 8 dBm (SMF) and 10 dBm (DCF), respectively. For 100 Gbit/s NRZ, this power increases to 17 dBm (SMF) and 19 dBm (DCF).

The nonlinear effect that has to be taken into account in the first place is self-phase modulation. The intensity of the signal itself leads to a nonlinear phase shift Φ_{NL} . Without dispersion, this phase shift is [49]

$$\Phi_{NL} = -\gamma P_0 L_{eff} \quad (2.35)$$

where P_0 is the peak power of the pulse propagating through the fiber with the effective length L_{eff} and the nonlinear index γ . The phase modulation of the complex fiber input envelope $A(0, t)$

$$A(L, t) = A(0, t)e^{i\Phi_{NL}} \quad (2.36)$$

leaves the amplitude unchanged. It leads to a chirp, though, modifying the carrier frequency by [49]

$$\Delta f = \frac{1}{2\pi} \gamma L_{eff} \frac{dP}{dt}. \quad (2.37)$$

⁶This modulation scheme has the lowest symbol rate of all 100 Gbit/s approaches discussed in chapter 1.

⁷NRZ has the highest symbol rate of the previously mentioned systems.

For slopes with power changes $dP/dt > 0$ this means blue shift and for slopes with $dP/dt < 0$ red shift. This phase modulation generates new spectral components broadening the signal spectrum.

Taking into account chromatic dispersion which converts phase modulation into amplitude modulation [8] SPM may lead to pulse compression as well as to pulse broadening. For positive dispersion $D > 0$, SPM first compresses the pulses by compensating for the higher propagation speed of the high frequency components of the pulse. With more accumulated dispersion, the pulse broadens less than without SPM. For $D < 0$, SPM leads to an enhanced pulse broadening by supporting the dispersion induced higher propagation speed for the low frequency components of the pulse.

2.3 Compensation of chromatic dispersion

Different approaches are followed to compensate the effect of chromatic dispersion. They can be distinguished in different ways:

- **Technology:** Optical compensation vs. Electronic compensation
- **Bandwidth:** Per-channel compensation vs. Full-band compensation
- **Flexibility:** Static compensation vs. Adaptive compensation

The main approaches are compared in Table 2.1. Today's most common method is the use of dispersion compensating fibers. The DCFs are not tunable and they are susceptible to nonlinearities. The insertion loss of the fiber requires also additional optical amplifiers. Chirped fiber bragg gratings on the other hand are tunable and have a low insertion loss. However, they have to be thermally stabilized and they show an inherent group delay ripple that may distort the signal. With manageable effort, these distortions can be electronically compensated [11].

For future systems, electronic equalization and optical filters are the options. Although first customers already deployed 40 Gbit/s and 100 Gbit/s links with electronic equalization, the complexity and the energy consumption is still an issue. Also commercially available are microoptical virtual image phased arrays (VIPAs) [7, 44]. However, these structures have in part a noticeable polarization dependency. This is not acceptable for polarization multiplexed systems used in 100 Gbit/s transmission. The tuning with micro optic lenses and mirror is complicated as well.

Despite of the fact that sophisticated dispersion compensators can replace the DCF spools, still in most of the systems they are deployed. For the foreseeable future, legacy and high bit rate channels will coexist on the deployed fiber infrastructure with static dispersion management. Fluctuations of the residual

dispersion e.g. due to environmental influence will make a residual dispersion compensation indispensable for high speed transmission channels. At these symbol rates the modulation format inherent dispersion tolerance is too small to tolerate these changes in chromatic dispersion. Following, delay line filters for residual dispersion compensation are discussed. Digital FIR as well as optical delay line filter realization options are compared. In the end, the realization in optical domain is focused.

Approach	Characterization	Advantages	Disadvantages
Dispersion Compensating Fibers	Optical compensation, full-band compensator, static	"Perfect" compensation of dispersion and dispersion slope possible, easy (passive) operation	Only static compensation is possible (need for additional residual dispersion compensation), high insertion loss causes use of additional optical amplifiers, nonlinearities may become an issue
Fiber-Bragg-Gratings	Optical compensation, available as per-channel and full-band compensator, tunable	Low insertion loss, high amounts of dispersion can be produced, can be placed at various locations in the network due to WDM capability and tunability	Group delay ripples are an inherent problem, higher line rates are more susceptible to that issue. FBGs have to be stabilized.

Table 2.1: Dispersion compensation methods

Approach	Characteriza- tion	Advantages	Disadvantages
Optical filters	Optical compensation, full-band, tunable, different technologies (arrayed waveguide gratings, photonic integrated circuits, optical delay line filters)	Tunability and WDM operation allow a broad field of operation, good energy efficiency	Still in development: stability is still an issue, tuning is complicated for higher filter orders
Digital filtering	Electronic per-channel equalization at the receiver	Mature technology known from wireless communications	Coherent detection needed for full performance, can only be placed at the receiver (per-channel equalization), high energy consumption, high data rates are challenging, modulation format specific

Table 2.2: Dispersion compensation methods (continued)

2.4 Delay Line Filters

Delay line filters are passive components based on the coherent superposition of incident fields. An incoming signal is split into different signal paths. These paths are delayed with respect to each other. Assuming that this relative delay length is shorter than the coherence length of the signal source⁸ the signal is superimposed with one or more delayed copies of itself. Feedback loops are also possible but this leads to infinite impulse response (IIR) type filters which is out of the scope of this work as they can not be realized in fiber optics⁹. However, the mathematical description and filter design process would be similar and can be easily extended to the feedback loop case.

2.4.1 Mathematical Description

In general terms, the input field

$$E_i = E_0(t)e^{j\omega t} \quad (2.38)$$

is split into up to $(N+1)$ different copies that are delayed individually by multiples of the unity delay $T_i = iT_0$ ($0 \leq i \leq N$). The unity delay T_0 defines the spectral periodicity of the filter called Free Spectral Range (FSR). The filter order N is determined by the highest delay $T_N = NT_0$. These copies of the input field E_i are finally recombined. The splitting and combining ratios determine the complex weighting coefficients¹⁰ b_i . The output field computes to

$$E_o = b_0 E_i + b_1 e^{j\omega T_1} E_i + b_2 e^{j\omega T_2} E_i + \dots \quad (2.39)$$

Thus, the filter transfer function $H(e^{j\omega}) = \frac{E_o}{E_i}$ can be written as

$$H(e^{j\omega}) = \sum_{i=0}^N b_i e^{j\omega iT_0} . \quad (2.40)$$

Setting $z = e^{-j\omega T_0}$ produces the standard description of a FIR filter in z -transform

$$H(z) = \sum_{i=0}^N b_i z^{-i} . \quad (2.41)$$

⁸This is easy to reach for all signal sources in optical communications. A typical DFB laser source has a coherence length of 1 - 100 m, ECLs even more, where delays usually are in the mm range.

⁹The free spectral range of IIR filters depends on the optical length of the feedback loop. For a FSR of 100 GHz, a circumference in the mm range is needed which is not possible to manufacture in fiber optics.

¹⁰ $|b_i| \leq 1$ for passive filters

Note that unlike for classical electrical FIR filters the filter coefficients b_i are complex here. It is worth mentioning that this representation can be used regardless of the way the electrical field is manipulated, i. e. the same description applies for optical delay line filters (direct manipulation of the electric field) and for electronic filters in conjunction with coherent detection (real and imaginary part of the field are manipulated separately in butterfly finite impulse response (FIR) filter structures).

2.4.2 Realization options

The analogy of delay line filters to FIR filters was already mentioned before. This type of filters can be realized in electrical domain as well as in optical domain. Using digital signal processing, the filters are regarded as complex-valued FIR filters. In optical domain, the same functionality can be achieved using optical delay line filters. The identical key characteristics are treated differently in electrical domain and in optical domain.

Frequency periodicity

Electronic FIR filters and optical delay line filters both show a frequency periodicity. For the digital FIR filters, the sampling rate of the symbol restricts the maximum frequency of the signal. Aliasing has to be avoided by applying band-pass or lowpass filters that limit the signal frequencies. On the other hand, for optical delay line filters the free spectral range also limits the maximum signal frequency. Higher frequency components would be filtered by the characteristics of the next “filter channel”. This can be interpreted as aliasing in the optical domain. It is worth mentioning that the length of the delay T_0 defines the spectral periodicity for electrical as well as for optical domain

$$\frac{1}{T_0} = f_{\text{sampling}} = FSR. \quad (2.42)$$

Bandwidth

The bandwidth of the filter transfer function is also equivalent: In electrical domain, oversampling results in using a lower bandwidth than the theoretically (Nyquist criterion) available one. The oversampling ratio OSR is defined as

$$OSR = \frac{f_{s,max}}{f_{max}} = \frac{2f_{s,max}}{f_{sampling}} \quad (2.43)$$

with the maximum signal frequency $f_{s,max}$ and the available maximum frequency $f_{max} = f_{sampling}/2$. In optical domain, the relative bandwidth used (RBWU) provides the same information using the optical bandwidth B_{opt}

$$RBWU = \frac{B_{opt}}{FSR} = \frac{2f_{s,max}}{f_{sampling}} = OSR. \quad (2.44)$$

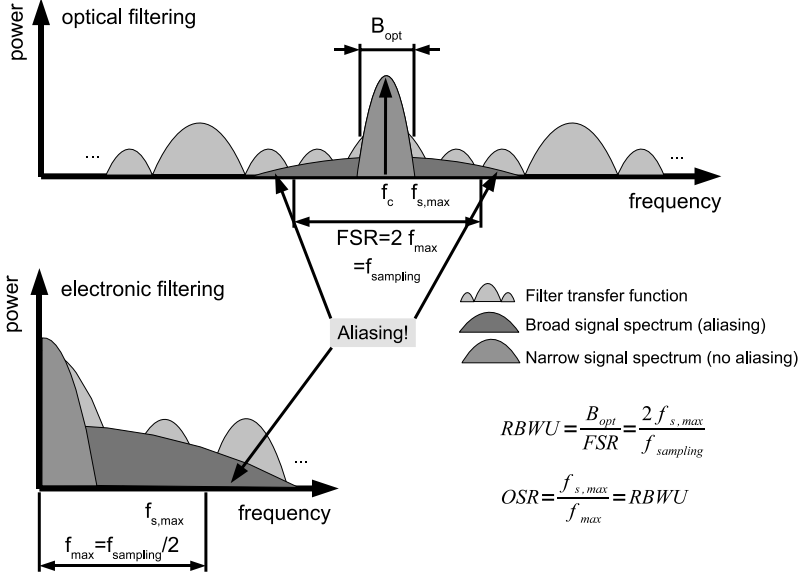


Figure 2.1: Analogy between optical filtering with delay line filters and electronic filtering with FIR filters

Electronic vs. optical filtering

Figure 2.1 illustrates the discussed analogy between optical and electronic filtering. However, in actual implementations, also some distinctions arise due to the different technologies. Usually, for optical delay line filters the FSR is set to the (ITU) grid of the WDM channels to take advantage of the multi channel capability of the optical delay line filters. Thus, depending on the modulation format, the required RBWU differs. On the other hand, oversampling is rarely used in electronic systems due to the enormous effort of high speed signal processing. Thus, in most cases sampling of two bits per symbol (Nyquist rate)

or even slightly below is applied. Therefore, the electronic filters should always provide a bandwidth of nearly 100%. On the other hand, this can be achieved more easily because filter orders in electronic filtering are usually higher than in optical filtering.

Electronic FIR filters are commonly used for single channel equalization after the receiving photo diode. The frequency periodicity is an unwanted feature that is suppressed by low pass filtering¹¹. Then again, the frequency periodicity of optical delay line filters is used to equalize different channels with one device taking advantage of the FSR being equal to the WDM grid. Aliasing or frequency mixing in the photo diode is prevented by the demultiplexing filter or heterodyne receiver architectures. Hence, the equivalent characteristics of digital FIR filtering and optical delay line filters are used differently according to the technological and economic framework of the application.

Although all considerations and all algorithms are valid for both kind of realizations due to the equivalence of digital FIR filtering and optical delay line filters the latter remain in focus here. The technological differences are the driving force of the specializations. However, obviously an adaptation to electronic filters will be easy if needed.

2.4.3 Realization in Optics

Optical delay line filters consist of optical couplers, optical phase shifters and optical delay lines. The signal is split and combined by the couplers with the complex coupling ratios κ . These coupling ratios equal the scattering parameter S_{ji} describing the relationship between the input port i and the output port j of the coupler.

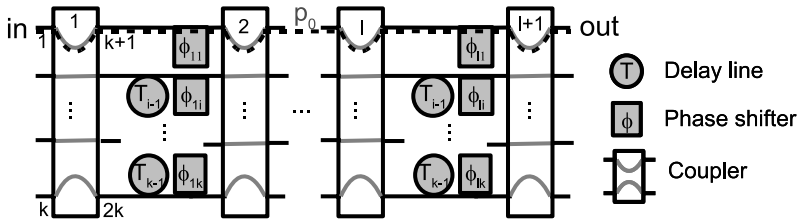


Figure 2.2: Structure of a general fiber optic delay line filter with $(l+1) \times k$ couplers (1 stages, k lines)

¹¹Often, the band limitation of the photo diode, the amplifiers and other electronic components redundantize an extra low pass aliasing filter.

For describing the physical transfer function of a general filter shown in Figure 2.2 using the S-parameters of the couplers, the phase shifters and the delay lines, a signal flow graph can be used. The S-parameters of the $k \times k$ couplers are named S_{ji}^m where $m = 1 \dots l + 1$ is the number of the coupler in the structure with l stages, $i = 1 \dots k$ are the input ports and $j = k + 1 \dots 2k$ are the output ports of the coupler. The general transfer function is constructed by multiplying the elements of the paths leading to a certain delay $z^{-\mu} = e^{j\omega\mu T_0}$ in the structure and summing the paths $p_{\mu,\nu}$ for the respective delays $z^{-\mu}$ up to the filter order N

$$H(z) = \sum_{\mu=0}^N \left(z^{-\mu} \sum_{\nu} p_{\mu,\nu} \right). \quad (2.45)$$

Please note that the sum of the paths determine the respective filter coefficient from equation (2.41)

$$b_{\mu} = \sum_{\nu} p_{\mu,\nu}. \quad (2.46)$$

For example, there is only one path in the structure (Figure 2.2) with no delay

$$b_0 = p_0 = S_{k+1,1}^{l+1} \prod_{m=1}^l S_{k+1,1}^m e^{j\varphi_{m1}}. \quad (2.47)$$

For more delay elements, there might be multiple paths (e.g. for one delay element it is possible to use the delay element in the first stage or the delay element in the second stage and so on).

If in every filter stage any possible delay $0, T_0, 2T_0, 3T_0, \dots$ is available the maximum filter order of the given structure is $N = (k - 1)l$. Trying to increase the filter order by providing not any delay in every filter stage decreases dramatically the possible transfer functions that can be realized with the filter due to cross dependencies of the S-parameters and the paths. That means, it is not possible any more to construct all filter coefficients b_0, b_1, \dots independently. Therefore, setting the delays $T_i = iT_0$ in the structure (Figure 2.2) is strongly recommended.

For the practical realization, two major structures are dominant: the serial one and the parallel one (Figure 2.3). Parallel filter structures are often realized as arrayed waveguide gratings¹² (AWG) [27]. The different paths are weighted with a phase profile [37]. The excitation of such a profile is very complex. Serial architectures are composed by connecting tunable Mach-Zehnder interferometers in series [4, 12, 16, 26, 48]. Per filter order, two quantities are needed to control the complex filter coefficients (absolute value and phase). Inceas-

¹²also called phased array (PHASAR)